REDISCUSSION OF ECLIPSING BINARIES. PAPER 31: THE SLOWLY-PULSATING B-STAR SYSTEM CV VELORUM IN THE *PLATO* SOUTHERN FIELD

By John Southworth

Astrophysics Group, Keele University, Staffordshire, ST5 5BG, UK

CV Vel is a detached eclipsing binary containing two B2·5 V stars in a circular orbit of period 6·889 d. Both stars show line-profile variations arising from g-mode oscillations, characteristic of slowly-pulsating B (SPB) stars, and rotational axes misaligned with the orbital axis. We present the first photometric analysis of the system based on light-curves from a space telescope. By combining our results with published spectroscopic observations we determine the stars' masses to be 6·065 ± 0·015 $M_\odot$ and 5·950 ± 0·012 $M_\odot$, and their radii to be 4·094 ± 0·056 $R_\odot$ and 3·978 ± 0·049 $R_\odot$. The precision of the radius measurements is limited by the pulsations in the light-curves. We identify two confirmed (0·4886 d^{-1} and 0·3695 d^{-1}) and two candidate (0·7468 d^{-1} and 0·7048 d^{-1}) pulsation frequencies but cannot reliably identify further frequencies due to the short duration of the available light-curves (approximately 50 d). CV Vel is in the first field to be observed by the *PLATO* satellite so in future may become the first EB containing an SPB star for which we have a light-curve with a high photometric precision and a duration of over one year.

Introduction

Eclipsing binaries (EBs) are our primary source of directly measured properties of normal stars[1,2] because their masses and radii can be measured to high precision and accuracy using only light- and radial-velocity (RV) curves[3]. Detached eclipsing binaries (dEBs) are of particular value as benchmarks against which the predictions of single-star evolutionary theory can be tested. The current work is part of a project[4] to reanalyse known dEBs using published spectroscopy and new space-based light-curves[5], for inclusion in the *Detached Eclipsing Binary Catalog*[6] (*DEBCat*[*]).

In this work we present an analysis of CV Velorum (Table I), which consists of two B2·5 V stars in an orbit of period 6·889 d. A rare — possibly unique — feature of CV Vel is that both stars belong to the class of slowly pulsating B stars. SPB stars are gravity-mode pulsators with masses of approximately 3 $M_\odot$ to 8 $M_\odot$ lying within the main-sequence band[7,8]. They show multi-periodic g-mode pulsations of high radial order and frequencies normally from 0·25 d^{-1} to 1 d^{-1}, excited by the heat-engine mechanism[9]. SPB pulsations can be used to constrain interior properties such as the efficiencies of mixing and angular-momentum transport[10,11].

Only a few SPB stars are known in dEBs: that list includes V539 Ara[12], μ Eri[13], AR Cas, and AS Cam (papers in preparation), and a few others found in surveys[14,15]. The combination of pulsations and eclipses is expected to lead to new insights into the physics governing the evolution of massive stars[16], but light-curves of sufficient duration (several years) to study SPB stars in EBs remain unavailable. That may soon change, because CV Vel is in the southern field of the forthcoming *PLATO* mission[17]. Here we present a photometric study

*https://www.astro.keele.ac.uk/jkt/debcat/

TABLE I

Basic information on CV Velorum. The BV magnitudes are each the mean of 151 individual measurements[18] distributed approximately randomly in orbital phase. The JHK_s magnitudes from 2MASS[19] were obtained at an orbital phase of 0·76.

Property	*Value*	*Reference*
Right ascension (J2000)	$09^h00^m37^s.99$	20
Declination (J2000)	$-51°33'20''.1$	20
Henry Draper designation	HD 77464	21
Tycho designation	TYC 8177-1750-1	18
Gaia DR3 designation	5323799125200766592	22
Gaia DR3 parallax (mas)	1·7652 ± 0·0333	22
TESS Input Catalog designation	TIC 401238440	23
B magnitude	6·507 ± 0·012	18
V magnitude	6·679 ± 0·012	18
J magnitude	6·963 ± 0·024	19
H magnitude	7·016 ± 0·033	19
K_s magnitude	7·061 ± 0·020	19
Spectral type	B2·5 V + B2·5 V	24

of CV Vel using space-based photometry, measuring pulsation frequencies in this object for the first time.

CV Velorum

CV Vel was discovered to be eclipsing by van Houten in 1950[25] in the course of a search for new variable stars using 18 photographic plates and a blink comparator. He found a period of 3·445 d and reported its spectral type to be B3.

Feast[26] discovered CV Vel to be a double-lined spectroscopic binary. He obtained the first spectroscopic orbit, based on 34 photographic spectra with reciprocal dispersions of 49 or 29 Å mm^{-1}, with a period of 6·892 d. That doubling of the orbital period is due to the primary and secondary eclipses being of very similar depth.

Gaposchkin[27] presented a photographic light-curve. He confirmed Feast's period measurement and, using Feast's RVs, provided the first determination of the masses and radii of the component stars.

Andersen[24] presented a spectroscopic study of CV Vel based on 32 photographic spectra[28] covering 3700–4700 Å with a reciprocal dispersion of 12·3 Å mm^{-1}. He found that "the two components appear virtually indistinguishable in both spectral type and luminosity" and adopted spectral types of B2·5 V for both. The lines were ideal for RV measurement due to their strength and low rotational broadening (given as 28 km s^{-1} ±10% for both components). Andersen measured RVs from 31 different absorption lines and demonstrated that line-blending causes an underestimation of the RVs of the stars measured from H and diffuse He lines. His final spectroscopic orbit rested on RVs from a set of ten strong and unblended lines arising from C, Ca, Si, Mg, and sharp He lines.

Clausen & Grønbech[29] observed CV Vel using the 50-cm Copenhagen telescope at ESO La Silla[30], obtaining complete coverage of the eclipses in the Strömgren u, b, v, and y bands. They found the secondary eclipse to occur slightly before phase 0·5, indicating a small but non-zero eccentricity. They modelled the data using the WINK code[31] and determined the masses and radii of the component stars. A light ratio of 0·90 ± 0·02, obtained on request by Andersen from his spectra, was used to constrain the light-curve solution and obtain a determinate value of the ratio of the radii of the stars.

Yakut *et al.*[32] obtained 30 high-quality échelle spectra of CV Vel and used them to determine new spectroscopic orbits and physical properties of the stars.* They found the secondary star (hereafter star B) to rotate faster than the primary (star A): $v_A \sin i = 31 \pm 2\,\mathrm{km\,s^{-1}}$ and $v_B \sin i = 19 \pm 1\,\mathrm{km\,s^{-1}}$. They also found both stars to show line-profile variations (stronger in star B than star A), with periods very uncertain but close to the orbital period. The physical properties of both stars are consistent with those of SPB stars. They found effective temperatures of 19000 ± 500 K and chemical abundances close to solar.

Finally, Albrecht *et al.*[33] obtained spectra of CV Vel during both eclipses to study the Rossiter–McLaughlin effect in the system[34,35]. They found star A to be misaligned with the orbit (sky-projected orbital obliquity $\beta = -52^\circ \pm 6^\circ$) and star B to be possibly aligned ($\beta = 3^\circ \pm 7^\circ$). In that model the precession of the spin axis of star A causes its $V \sin i$ to vary with a period of approximately 140 yr. The observed change in the rotational broadening of star B suggests it too has a significant true orbital obliquity, and that the measurement of β happened at a time when the sky-projection of the obliquity was low.

Photometric observations

CV Vel has been observed by the *Transiting Exoplanet Survey Satellite* (*TESS*[36]) mission in eight sectors so far, with a range of cadences. Sectors 8 and 9 were observed at 1800-s cadence; 35, 36, 89, and 90 at 600-s cadence; and 62 and 63 at 200-s cadence. We used the LIGHTKURVE package[37] to download the light-curves for all sectors from the *Mikulski Archive for Space Telescopes* (*MAST*†). Light-curves from the *TESS* Science Processing Center (SPOC[38]) are available for sectors 62 and 63, whereas only QUICK LOOK PIPELINE (QLP[39]) data are available for the other sectors.

We converted the light-curves from flux into differential magnitudes, specified the 'hard' option to reject data of lower quality, and subtracted the median magnitude from each sector. The results are plotted in Fig. 1, where eclipses and pulsations are both visible. We based most of our analysis on sectors 62 and 63 because of the higher time resolution of the data.

CV Vel is close to the Galactic plane so is in a relatively rich star field. A query of the *Gaia* DR3 database‡ returns a total of 405 sources within 2 arcmin of CV Vel and thus potential contaminants of the *TESS* light-curve. The brightest of those in the *Gaia* $G_{\rm RP}$ band, a red passband tolerably well matched to the *TESS* response function, is fainter by 4·46 mag. The fainter stars are relatively evenly spread so will be removed by the sky-subtraction step in the reduction of the *TESS* data. We therefore expect the amount of contaminating light in the *TESS* light-curve of CV Vel to be small but not zero.

Light-curve analysis

We concentrated our analysis on the light-curve formed by combining *TESS* sectors 62 and 63, totalling 21 746 data points, which have a higher time resolution than the rest of the data. The two stars are well-detached so are suitable for analysis with the JKTEBOP§ code[40,41], for which we used version 45. We fitted for the orbital period (P), a reference time of primary minimum (T_0; when star A is eclipsed by star B) close to the midpoint of the data, the sum ($r_A + r_B$) and ratio ($k = r_B/r_A$) of the fractional radii, the central-surface-brightness ratio (J), third light (L_3), and orbital inclination (i).

We included limb darkening (LD) using the power-2 law[42–44], using the same coefficients for both stars due to their extreme similarity. The linear coefficient (c) was fitted and the nonlinear coefficient (α) was fixed at a theoretical value[45,46]. We tested for the presence

*Note that Yakut *et al.*[32] switched the identities of the two stars[33]. Their results quoted in the current work have been updated to account for that.

†https://mast.stsci.edu/portal/Mashup/Clients/Mast/Portal.html

‡https://vizier.cds.unistra.fr/viz-bin/VizieR-3?-source=I/355/gaiadr3

§http://www.astro.keele.ac.uk/jkt/codes/jktebop.html

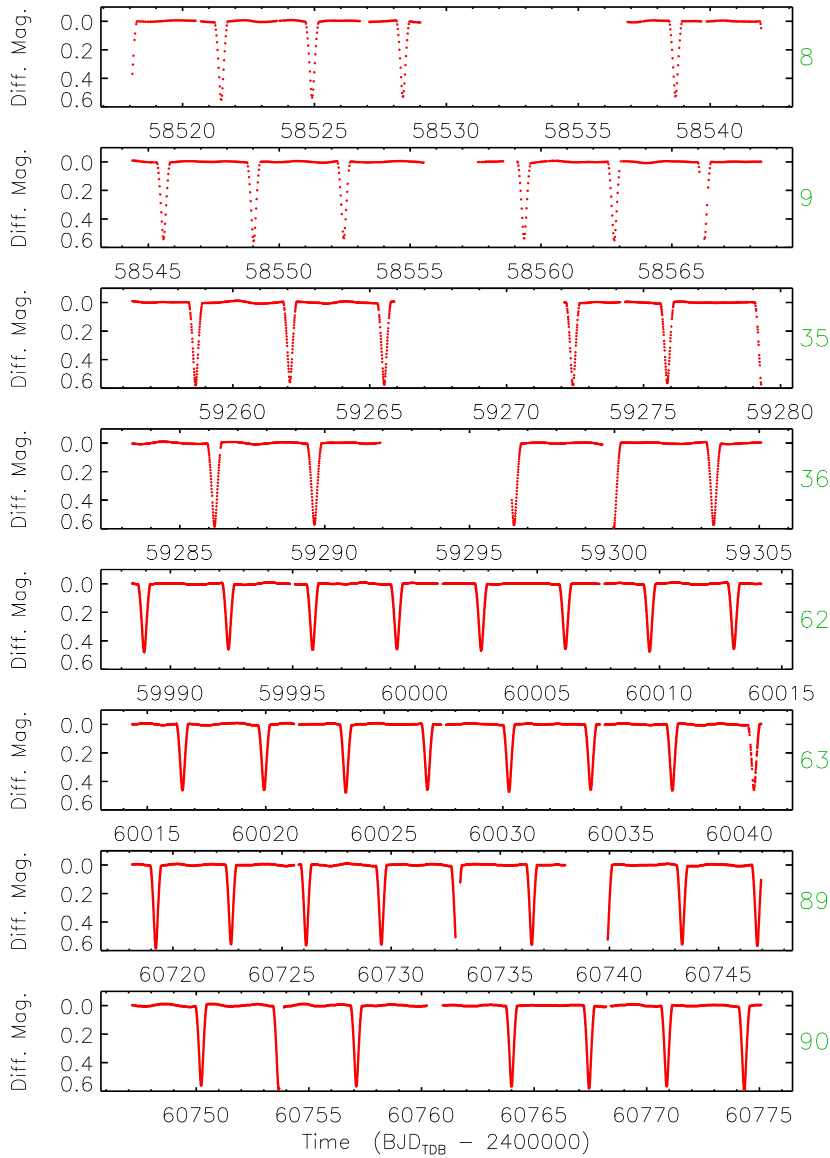

FIG. 1

Light-curves of CV Vel from all eight *TESS* sectors. The flux measurements have been converted to magnitude units and the median subtracted.

of orbital eccentricity and found no substantive evidence, so assumed a circular orbit. The pulsations in the light-curve are of much greater amplitude than caused by effects such as which LD law to use and whether to include eccentricity, so our ability to tease out those

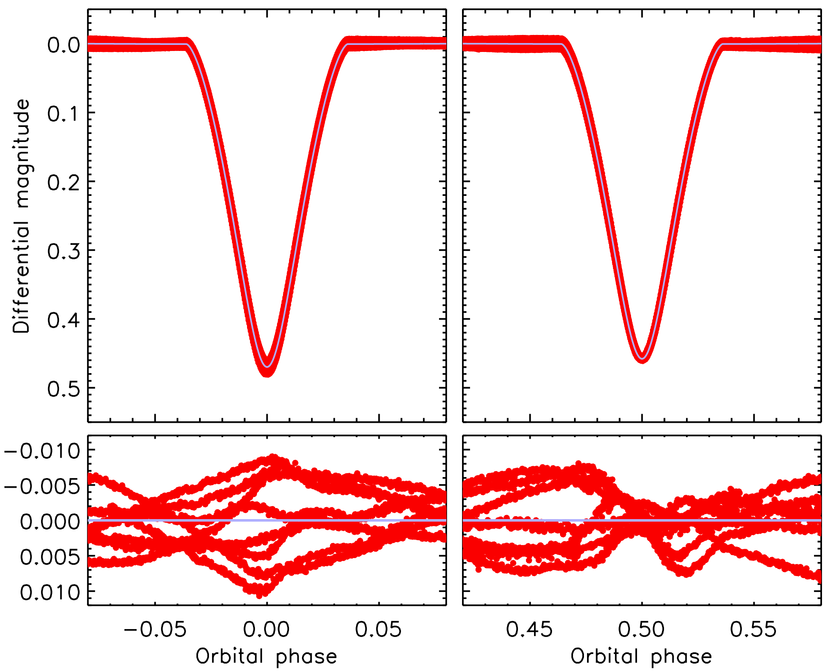

FIG. 2

JKTEBOP best fit to the light-curves of CV Vel from *TESS* sectors 62 and 63 for the primary eclipse (left panels) and secondary eclipse (right panels). The data are shown as filled red circles and the best fit as a light-blue solid line. The residuals are shown on an enlarged scale in the lower panels, and are dominated by the pulsations.

subtleties from the data is limited.

The best fit to the light-curve is insensitive to k, as previously noted for this system[29]. We followed Clausen & Grønbech in specifying a light ratio of 0·90 ± 0·02 measured by Andersen from two spectra of the system at quadrature. That light ratio was obtained at blue wavelengths but was applied directly in our JKTEBOP model of the much redder *TESS* data because the two stars have almost identical temperatures. We found that that light ratio gives a significant improvement in the determinacy of our light-curve model. For illustration, in Table II we give the best-fitting parameters with and without the inclusion of that light ratio. The amount of third light is small and consistent with zero, as expected.

We were able to obtain a good fit to the eclipses (Fig. 2). The residuals are dominated by the pulsations, which are at a maximum at the midpoint of primary eclipse and a minimum at the midpoint of secondary eclipse. As star A dominates the light of the system during secondary eclipse and is mostly obscured during primary eclipse, we deduce that the dominant pulsations in the light-curve arise from star B. That agrees with previous observations of stronger line-profile variability in star B than star A[32,33].

We determined the uncertainties in the fitted parameters using the residual-permutation algorithm implemented as Task 9 in JKTEBOP[47], thus treating the pulsations as correlated noise. There was no point conducting our usual Monte Carlo simulations as that algorithm assumes the data contain only the eclipse model and white noise. The best-fitting parameters and uncertainties are given in Table II. The uncertainties we find are driven by the pulsations, and are larger than those in recent publications[32,33]. Our orbital-inclination measurement agrees well with that from Clausen & Grønbech[29], so there is no evidence for changes in that parameter as might be caused by precession of the rotational axes[33].

We considered adding the *TESS* data from sectors 35, 36, 89, and 90 to this analysis, to average out the effect of the pulsations and potentially allow more-precise measurements of the properties in Table II. However, those data show much deeper eclipses (0·59 mag) than those from sectors 62 and 63 (0·48 mag) so it is not straightforward to combine them. Previous light-curves of CV Vel show eclipse depths in agreement with those from sectors 62 and 63, so we conclude that the different data-reduction procedures for QLP *versus* SPOC give an incorrect light-curve scaling. We have seen that before for other dEBs.

We then attempted to lower the error bars in Table II by removing the majority of the pulsational effects from the light-curve. We used PERIOD04 (see below) to fit and subtract 11 frequencies which plausibly exist, then refitted the light-curve with JKTEBOP. That gave a much improved fit but only a small change in some of the fitted light-curve parameters. The solution prefers a higher light ratio than that measured by Andersen, giving a ratio of the radii that is closer to unity and less consistent with expectations from stellar evolutionary theory. That new fit is also given in Table II for reference, but we did not use its results in the remainder of our analysis.

Orbital ephemeris

We calculated an improved orbital ephemeris based only on the *TESS* data. We fitted each pair of adjacent *TESS* sectors with JKTEBOP to obtain one effective time of primary eclipse per pair of sectors. Those are given in Table III. A straight-line fit to those data returns the following linear ephemeris:

$$\text{Min I} = \text{BJD}_\text{TDB}\ 2460009{\cdot}59629(6) + 6{\cdot}8894985(4)E \qquad (1)$$

where E is the number of cycles since the reference time of minimum and the bracketed quantities indicate the uncertainty in the final digit of the previous number. The scatter around the best fit is slightly larger than the error bars suggest, with a reduced χ^2 of $\chi^2_\nu = 1{\cdot}2$, so the uncertainties in the ephemeris have been multiplied by $\sqrt{\chi^2_\nu}$ to account for that. There is no evidence for a change in the orbital period based on those data, albeit over a small time interval. Further historical times of minimum exist, as do more recent survey data, which could be used for a more extensive search for orbital period changes.

Physical properties and distance to CV Vel

We determined the physical properties of CV Vel using our results from the light-curve analysis above (r_A, r_B, i, and P from Table II) and the JKTABSDIM code[48]. To those we added the velocity amplitudes of $K_\text{A} = 126{\cdot}69 \pm 0{\cdot}11$ km s^{-1} and $K_\text{B} = 129{\cdot}15 \pm 0{\cdot}11$ km s^{-1} from Albrecht *et al.*[33], adding the quoted statistical and systematic errors in quadrature to give a single error bar for each quantity. The temperatures of the stars were taken from Torres *et al.*[2], which are representative of most values quoted in the literature. The results are given in Table IV.

To measure the distance to the system we used the parameters above, the BV magnitudes from *Tycho*[18] and JHK_s magnitudes from 2MASS[19] given in Table I, and bolometric corrections from Girardi *et al.*[50]. A reddening of $E(B-V) = 0{\cdot}06 \pm 0{\cdot}02$ mag brought the distances in the BV passband into alignment with those in JHK_s. That led to a final distance measurement in the K_s band (which is least affected by reddening) of 568 ± 10 pc, in excellent agreement with the distance of 567 ± 11 pc from inversion of the *Gaia* DR3 parallax.

The age of the system was estimated by comparing the measured masses, radii, and temperatures to theoretical predictions from the PARSEC 1.2 evolutionary models[51]. We

TABLE II

Photometric parameters measured using JKTEBOP *from the light-curve of CV Vel from TESS sectors 62+63. The error bars are 1-σ and are calculated from residual-permutation simulations. The adopted solution is the first one.*

Parameter	ℓ_B/ℓ_A *constrained*	ℓ_B/ℓ_A *not constrained*	*With 11 frequencies removed*
Fitted parameters:			
Orbital period (d)	6·889466 ± 0·000056	6·889466 ± 0·000056	6·889488 ± 0·000027
Time of primary eclipse (BJD_{TDB})	2460009·59623 ± 0·00011	2460009·59623 ± 0·00011	2460009·59618 ± 0·00011
Orbital inclination (°)	86·652 ± 0·012	86·636 ± 0·051	86·645 ± 0·017
Sum of the fractional radii	0·2313 ± 0·0009	0·2315 ± 0·0008	0·2319 ± 0·0008
Ratio of the radii	0·971 ± 0·024	1·016 ± 0·091	1·009 ± 0·018
Central-surface-brightness ratio	0·9793 ± 0·0048	0·9792 ± 0·0048	0·9791 ± 0·0014
Third light	−0·0023 ± 0·0073	0·0000 ± 0·0065	0·0036 ± 0·0065
LD coefficient c	0·46 ± 0·11	0·49 ± 0·07	0·53 ± 0·08
LD coefficient α	0·3591 (fixed)	0·3591 (fixed)	0·3591 (fixed)
Derived parameters:			
Fractional radius of star A	0·1173 ± 0·0016	0·1148 ± 0·0072	0·1154 ± 0·0012
Fractional radius of star B	0·1140 ± 0·0014	0·1167 ± 0·0051	0·1164 ± 0·0012
Light ratio ℓ_B/ℓ_A	0·924 ± 0·042	1·01 ± 0·17	0·996 ± 0·035

TABLE III

Times of mid-eclipse for CV Vel and their residuals versus the fitted ephemeris.

Orbital cycle	*Eclipse time (BJD_{TDB})*	*Uncertainty (d)*	*Residual (d)*	*TESS sectors*
−212·0	2458549·02243	0·00013	−0·00018	08, 09
−105·0	2459286·19909	0·00009	0·00015	35, 36
0·0	2460009·59623	0·00011	−0·00006	62, 63
107·0	2460746·77262	0·00006	−0·00001	89, 90

TABLE IV

Physical properties of CV Vel defined using the nominal solar units given by IAU 2015 Resolution B3 (ref. 49).

Parameter	*Star A*	*Star B*
Mass ratio $M_{\rm B}/M_{\rm A}$	0·9810 ± 0·0014	
Semimajor axis of relative orbit ($\mathcal{R}^{\rm N}_{\odot}$)	34·899 ± 0·025	
Mass ($\mathcal{M}^{\rm N}_{\odot}$)	6·065 ± 0·015	5·950 ± 0·012
Radius ($\mathcal{R}^{\rm N}_{\odot}$)	4·094 ± 0·056	3·978 ± 0·049
Surface gravity (log[cgs])	3·997 ± 0·012	4·013 ± 0·012
Density ($\rho_{\odot}$)	0·0884 ± 0·0036	0·0945 ± 0·0035
Synchronous rotational velocity (km s^{-1})	30·06 ± 0·41	29·22 ± 0·36
Effective temperature (K)	18100 ± 500	17900 ± 500
Luminosity $\log(L/\mathcal{L}^{\rm N}_{\odot})$	3·210 ± 0·049	3·166 ± 0·049
$M_{\rm bol}$ (mag)	−3·28 ± 0·12	−3·17 ± 0·13
Interstellar reddening $E(B-V)$ (mag)	0·06 ± 0·02	
Distance (pc)	568·4 ± 9·5	

found an essentially perfect fit for an age of 40 ± 1 Myr assuming a solar metal abundance fraction by mass of Z = 0·017. A lower metal abundance of Z = 0·014 gives a slightly worse fit (but still well within the error bars) for an age older by 3 Myr. Similarly, a higher metal abundance of Z = 0·020 leads to a preference for an age younger by only 1 Myr.

Pulsation analysis

The *TESS* light-curve of CV Vel shows clear evidence for multi-periodic pulsations (see Fig. 3), as expected from the prior detections of line-profile variations in both stars[32,33]. We combined the eight *TESS* sectors into four pairs, fitted and subtracted a JKTEBOP model, then calculated frequency spectra for each pair of sectors using version 1.2.0 of the PERIOD04 code[52]. Those are shown in Fig. 4.

All four pairs of sectors show the strong detection of an oscillation with a frequency of f_1 = 0·4886 d^{-1}, an amplitude of 3·8 mmag, and a signal-to-noise ratio* (S/N) of 9·5. In the current paragraph we quote results from the data from sectors 62 and 63 as it has the lowest noise of the four pairs of sectors. A second frequency at f_2 = 0·3695 d^{-1} and amplitude 1·6 mmag is detected with a S/N of only 3·6, lower than needed for confirmed signals[53], but its presence in all four sector pairs supports its reality. Two further candidate frequencies, f_3 = 0·7468 d^{-1} (amplitude 0·9 mmag) and f_4 = 0·7048 d^{-1} (amplitude 0·7 mmag) are detected with S/N values of 2·9 and 2·7, respectively. f_3 and f_4 are each visible in three of the four sector pairs so are likely real but not confirmable with the currently available data.

*The S/N is the ratio of the height of the peak to the mean signal within an interval of 2 d^{-1} centred on the peak.

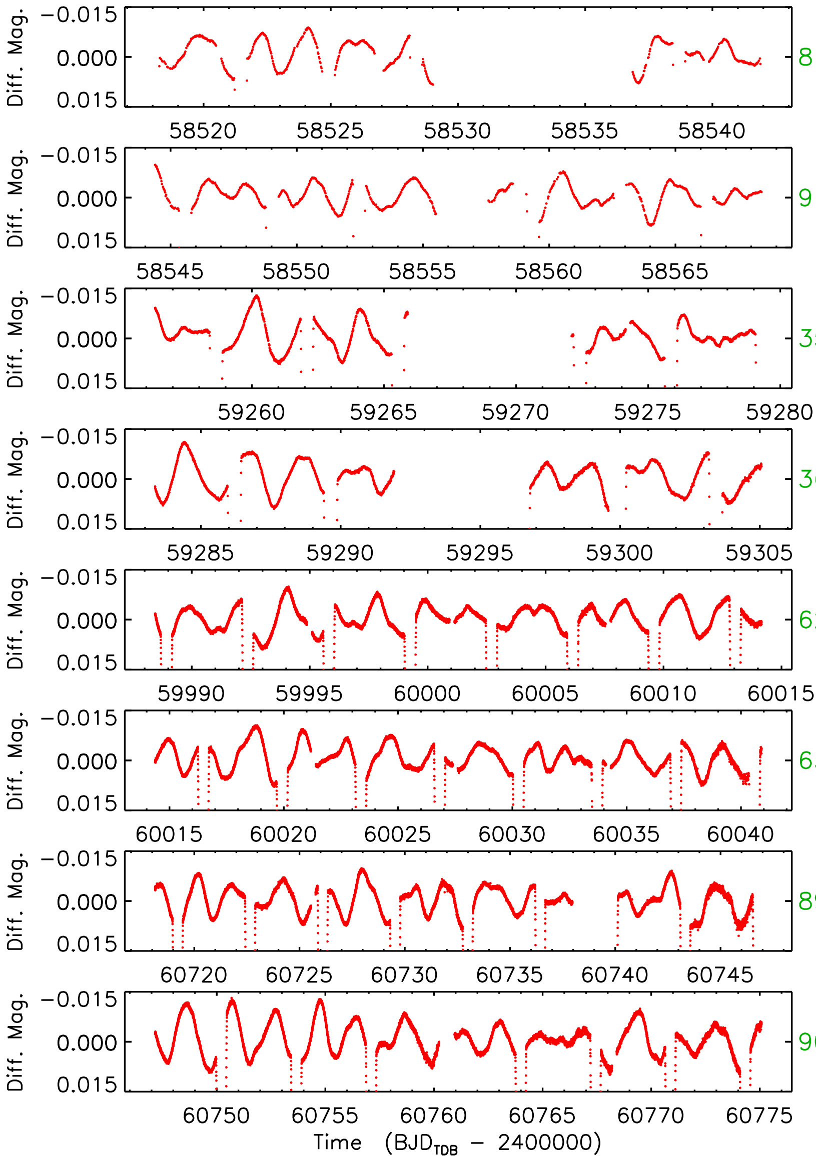

Fig. 3
Same as Fig. 1 but with the ordinate axis enlarged to make the pulsations clearer.

We did not see any peaks in the frequency spectrum near multiples of the orbital frequency. We also checked and found no significant frequencies from $1{\cdot}1\,d^{-1}$ out to the Nyquist limit of $215\,d^{-1}$.

The confirmed and tentative frequency detections all lie at low frequencies, in a range

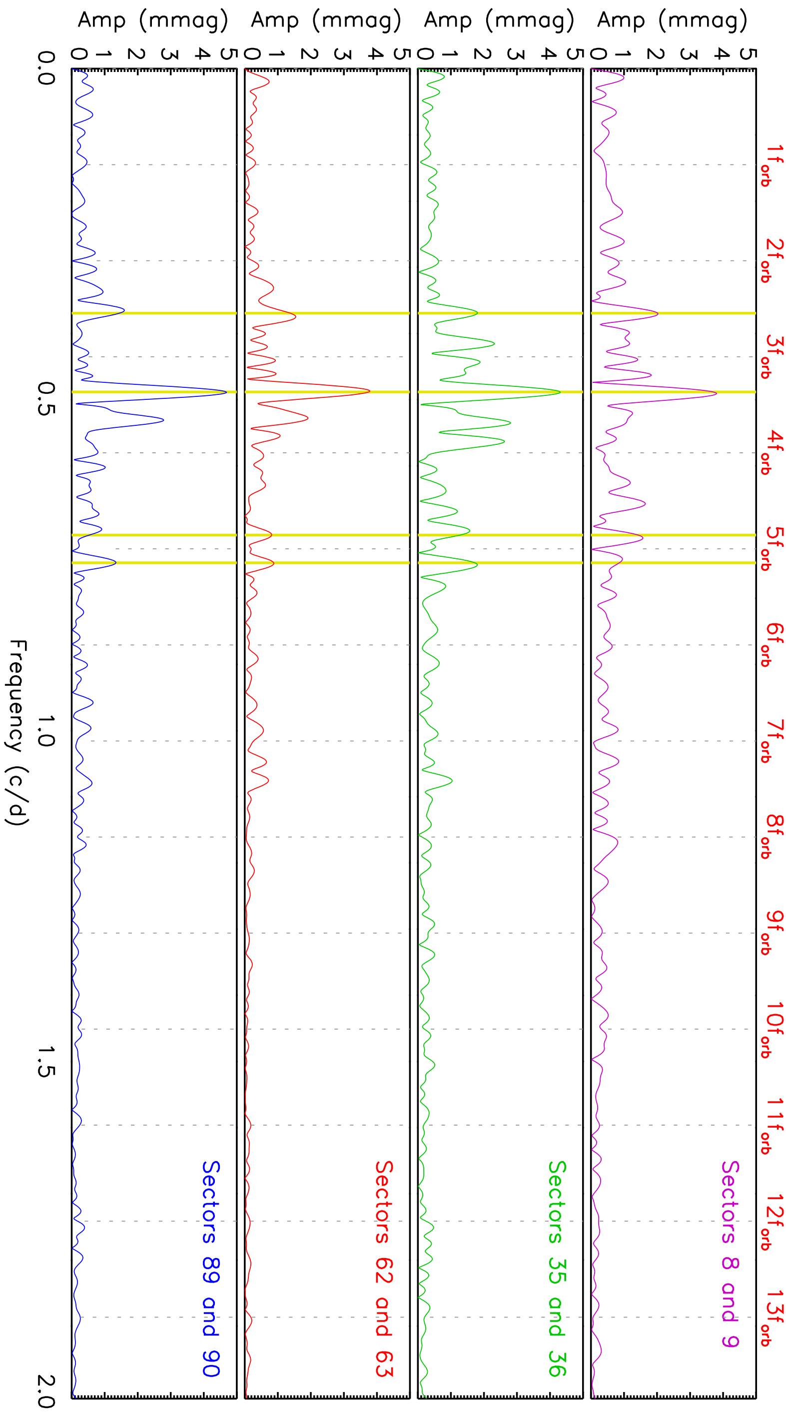

Fig. 4

Frequency spectra of CV Vel from the four pairs of *TESS* sectors (labelled in the top-right of each panel). The frequency spectra are plotted with coloured lines. Multiples of the orbital frequency are plotted with grey dashed lines and annotated at the top of the plot. The four frequencies discussed in the text are indicated with thick yellow lines.

characteristic of the SPB pulsators[8,14]. The properties of both stars are also inside and close to the hotter boundary for which SPB pulsations are expected[9]. As both stars show line-profile variations, we conclude that they are both SPB pulsators. We defer a detailed frequency analysis until light-curves of much longer duration are available in future.

Summary and conclusions

CV Vel is a dEB containing two almost-identical B2·5 V stars in a circular orbit of period 6·889 d. We have determined the masses and radii of the stars based on published spectroscopic studies and an analysis of light-curves from the *TESS* mission. The pulsations in the light-curve prevented us from determining the radii of the stars to high precision. We found a distance in good agreement with the parallax from *Gaia* DR3, and an age of 40 Myr from comparison with theoretical models. The rotational axes of both stars are misaligned with the orbital axis, and are precessing with periods of centuries. Due to that, the projected rotational velocities of the stars change over time.

Both stars are known to show line-profile variations indicative of pulsations of the SPB type. We have presented the first photometric detection of SPB pulsations and measured two certain and two tentative frequencies in the range 0·37 d^{-1} to 0·75 d^{-1}. Additional variability is visible in the frequency spectrum but no further frequencies are reliably detected in the available data. CV Vel is in the southern field (LOPS2[54,55]) of the *PLATO* mission[17], which is scheduled for launch in early 2027 and will observe that field for (at least) the first two years of its mission. Observations of CV Vel from *PLATO* will allow a much more detailed analysis of the radii and pulsation frequencies of the star, and we will be proposing it as a high-priority target in the *PLATO* Guest Observer programme[*].

Acknowledgements

We thank the anonymous referee for a helpful report. We acknowledge support from STFC under grant number ST/Y002563/1. This paper includes data collected by the *TESS* mission and obtained from the *MAST* data archive at the Space Telescope Science Institute (STScI). Funding for the *TESS* mission is provided by the NASA's Science Mission Directorate. STScI is operated by the Association of Universities for Research in Astronomy, Inc., under NASA contract NAS 5-26555. This paper includes observations made with the *Isaac Newton Telescope* operated on the island of La Palma by the Isaac Newton Group of Telescopes in the Spanish Observatorio del Roque de los Muchachos of the Instituto de Astrofísica de Canarias. This work has made use of data from the European Space Agency (ESA) mission *Gaia*[†], processed by the *Gaia* Data Processing and Analysis Consortium (DPAC[‡]). Funding for the DPAC has been provided by national institutions, in particular the institutions participating in the *Gaia* Multilateral Agreement. The following resources were used in the course of this work: the NASA Astrophysics Data System; the *Simbad* database operated at CDS, Strasbourg, France; and the arχiv scientific-paper preprint service operated by Cornell University.

References

(1) J. Andersen, *A&ARv*, **3**, 91, 1991.
(2) G. Torres, J. Andersen & A. Giménez, *A&ARv*, **18**, 67, 2010.
(3) P. F. L. Maxted *et al.*, *MNRAS*, **498**, 332, 2020.
(4) J. Southworth, *The Observatory*, **140**, 247, 2020.

*https://www.cosmos.esa.int/web/plato/guest-observers

†https://www.cosmos.esa.int/gaia

‡https://www.cosmos.esa.int/web/gaia/dpac/consortium

(5) J. Southworth, *Universe*, **7**, 369, 2021.
(6) J. Southworth, in *Living Together: Planets, Host Stars and Binaries* (S. M. Rucinski, G. Torres & M. Zejda, eds.), 2015, *Astronomical Society of the Pacific Conference Series*, vol. 496, p. 321.
(7) C. Waelkens & F. Rufener, *A&A*, **152**, 6, 1985.
(8) C. Waelkens, *A&A*, **246**, 453, 1991.
(9) W. A. Dziembowski, P. Moskalik & A. A. Pamyatnykh, *MNRAS*, **265**, 588, 1993.
(10) M. G. Pedersen *et al.*, *Nature Astronomy*, **5**, 715, 2021.
(11) M. G. Pedersen, *ApJ*, **940**, 49, 2022.
(12) J. V. Clausen, *A&A*, **308**, 151, 1996.
(13) M. Jerzykiewicz *et al.*, *MNRAS*, **432**, 1032, 2013.
(14) J. Southworth & D. M. Bowman, *MNRAS*, **513**, 3191, 2022.
(15) Ö. Çakırlı, B. Hoyman & O. Özdarcan, *MNRAS*, **544**, 607, 2025.
(16) J. Southworth & D. Bowman, *ARA&A, in press,* `arXiv:2509.08426`, 2026.
(17) H. Rauer *et al.*, *Experimental Astronomy*, **59**, 26, 2025.
(18) E. Høg *et al.*, *A&A*, **355**, L27, 2000.
(19) R. M. Cutri *et al.*, *2MASS All Sky Catalogue of Point Sources* (The IRSA 2MASS All-Sky Point Source Catalogue, NASA/IPAC Infrared Science Archive, Caltech, US), 2003.
(20) Gaia Collaboration, *A&A*, **674**, A1, 2023.
(21) A. J. Cannon & E. C. Pickering, *Annals of Harvard College Observatory*, **94**, 1, 1919.
(22) Gaia Collaboration, *A&A*, **649**, A1, 2021.
(23) K. G. Stassun *et al.*, *AJ*, **158**, 138, 2019.
(24) J. Andersen, *A&A*, **44**, 355, 1975.
(25) C. J. van Houten, *Annalen van de Sterrewacht te Leiden*, **20**, 223, 1950.
(26) M. W. Feast, *MNRAS*, **114**, 246, 1954.
(27) S. Gaposchkin, *MNRAS*, **115**, 391, 1955.
(28) J. Andersen, *A&A*, **44**, 445, 1975.
(29) J. V. Clausen & B. Grønbech, *A&A*, **58**, 131, 1977.
(30) B. Grønbech, E. H. Olsen & B. Strömgren, *A&AS*, **26**, 155, 1976.
(31) D. B. Wood, *AJ*, **76**, 701, 1971.
(32) K. Yakut, C. Aerts & T. Morel, *A&A*, **467**, 647, 2007.
(33) S. Albrecht *et al.*, *ApJ*, **785**, 83, 2014.
(34) R. A. Rossiter, *ApJ*, **60**, 15, 1924.
(35) D. B. McLaughlin, *ApJ*, **60**, 22, 1924.
(36) G. R. Ricker et al., *Journal of Astronomical Telescopes, Instruments, and Systems*, **1**, 014003, 2015.
(37) Lightkurve Collaboration, *Lightkurve: Kepler and TESS time series analysis in Python*, Astrophysics Source Code Library, 2018.
(38) J. M. Jenkins *et al.*, in *Proc. SPIE*, 2016, *Society of Photo-Optical Instrumentation Engineers (SPIE) Conference Series*, vol. 9913, p. 99133E.
(39) C. X. Huang *et al.*, *RNAAS*, **4**, 204, 2020.
(40) J. Southworth, P. F. L. Maxted & B. Smalley, *MNRAS*, **351**, 1277, 2004.
(41) J. Southworth, *A&A*, **557**, A119, 2013.
(42) D. Hestroffer, *A&A*, **327**, 199, 1997.
(43) P. F. L. Maxted, *A&A*, **616**, A39, 2018.
(44) J. Southworth, *The Observatory*, **143**, 71, 2023.
(45) A. Claret & J. Southworth, *A&A*, **664**, A128, 2022.
(46) A. Claret & J. Southworth, *A&A*, **674**, A63, 2023.
(47) J. Southworth, *MNRAS*, **386**, 1644, 2008.
(48) J. Southworth, P. F. L. Maxted & B. Smalley, *A&A*, **429**, 645, 2005.
(49) A. Prša *et al.*, *AJ*, **152**, 41, 2016.
(50) L. Girardi *et al.*, *A&A*, **391**, 195, 2002.
(51) A. Bressan *et al.*, *MNRAS*, **427**, 127, 2012.
(52) P. Lenz & M. Breger, *Communications in Asteroseismology*, **146**, 53, 2005.
(53) A. S. Baran & C. Koen, *AcA*, **71**, 113, 2021.
(54) V. Nascimbeni *et al.*, *A&A*, **658**, A31, 2022.
(55) V. Nascimbeni *et al.*, *A&A*, **694**, A313, 2025.